

Glenosphere Posterior Eccentricity Effect on Range of Motion and Anterior Impingement in Reverse Shoulder Arthroplasty in a Virtual Model. A Study of La Tour Group.

Alberto Guizzi¹, Patrick J. Denard², Philippe Collin^{3 4 5}, Alaa Elsenbsy^{6 7}, Anthony Pernoud⁹, Hugo Bothorel⁹, Alexandre Lädermann^{6 8 10 11} (*)

(*) Corresponding author: alexandre.laedermann@gmail.com

1. Department of Medical and Surgical Specialties, Radiological Sciences, and Public Health, University of Brescia, Piazza del Mercato 15, 25121, Brescia, Italy

2. Oregon Shoulder Institute, Medford, Oregon, U.S.A.

3. CHP Saint-Grégoire, 6 boulevard de la Boutière, 35760 Saint-Grégoire, France

4. Clinique Victor Hugo, 5 bis rue du Dôme, 75016 Paris, France

5. American Hospital of Paris, 55 boulevard du château, 92200 Neuilly-sur-Seine, France

6. Division of Orthopaedics and Trauma Surgery, Hôpital de La Tour, Rue J.-D. Maillard 3, 1217 Meyrin, Switzerland

7. Department of Orthopedic and Trauma Surgery, Faculty of Medicine, South Valley University, Qena, Egypt

8. Faculty of Medicine, University of Geneva, Rue Michel-Servet 1, 1211 Geneva 4, Switzerland

9. Department of Research, Hôpital de La Tour, Rue J.-D. Maillard 3, 1217 Meyrin, Switzerland

10. Division of Orthopaedics and Trauma Surgery, Department of Surgery, University Hospitals, Rue Gabrielle-Perret-Gentil 4, 1211 Geneva 14, Switzerland

11. FORE (Foundation for Research and Teaching in Orthopedics, Sports Medicine, Trauma, and Imaging in the Musculoskeletal System), Avenue J.-D. Maillard 3, 1217 Meyrin, Switzerland



Background: Reverse shoulder arthroplasty (RSA) improves outcomes in cuff-deficient shoulders, but internal rotation recovery and anterior impingement remain inconsistent. While inferior placement and eccentric glenospheres may enhance motion, the role of posterior eccentricity in impingement and multiplanar function is unclear.

Purpose: This study evaluated the effect of glenoid lateralization and posterior eccentricity in RSA on impingement-free ROM, hypothesizing that posterior eccentricity would enhance Hand-Behind-Back motion and reduce anterior impingement.

Methods: CT scans obtained in 13 patients (3 men and 10 women) with A1 primary osteoarthritis were analyzed using a three-dimensional (3D) computer model simulating implantation of a standardized RSA. A 135° inlay humeral component and the combination of four different glenoid-sided variables were analyzed: glenoid lateralization (0, 3, and 6 mm), 36 mm glenosphere eccentricity (concentric, posteroinferior (45°), and posterior (90°)). ROM, impingement, and the implant distance to the coracoid and conjoint tendon were recorded in each scenario.

Results: Positioning the glenosphere 5 mm inferior to the glenoid rim resulted in significantly increased ROM: +51% in hand-to-contralateral motion, +26° in external rotation, and +52° in extension ($p < 0.001$), compared to a flush glenosphere. Inferior glenospheres were further from the coracoid process by 2.6 mm but slightly closer to the conjoint tendon by 0.7 mm. Posteroinferior and posterior eccentricities enhanced extension (+18°) and external rotation (+5°), but decreased internal rotation (-5° to -11°) and hand-to-contralateral motion (-8% to -28%) ($p < 0.05$). Posteroinferior and posterior eccentricities also increased the distance from the coracoid process by 1.3–1.6 mm and from the conjoint tendon by 1.1–1.3 mm ($p < 0.05$).

Conclusion: In a virtual RSA model with a 135° inlay humeral component, posteroinferior eccentricity with lateral offset optimized ROM, including HBB, and may reduce anterior impingement by increasing coracoid and conjoint tendon clearance.

What this study adds: This study shows that in a virtual RSA model, posteroinferior/posterior glenosphere eccentricities with inferior positioning and lateral offset improved motion and clearance, potentially reducing anterior impingement and supporting implant optimization.

Potential impacts on research, practice or policy: This study demonstrates that posterior or posteroinferior eccentricity with inferior positioning and lateral offset can enhance ROM and reduce anterior impingement, guiding implant strategies to optimize outcomes.

Study design: Basic Science Study; Computer Modeling

Keywords: Prosthesis; Implant configuration; Eccentric; PROMs; Reverse Shoulder Arthroplasty

<https://doi.org/10.70885/hmsj.2025.09.003>

Introduction

Reverse shoulder arthroplasty (RSA) has shown progressively better functional outcomes over time, thanks to improved surgical skills and technology improvements [1][2]. However, complications remain; amongst them, unpredictable recovery of internal rotation [3] and anterior impingement [4]. Numerous strategies have been described to improve internal rotation including modifications of the prosthetic design [5], glenoid lateralization [6][7], and subscapularis repair [3] or preservation [8][9]. Computer [10][11] and clinical [12] studies have explored inferior glenosphere eccentricity or posteroinferior glenosphere positioning on postoperative range of motion (ROM). At the same time, anterior impingement, an under reported phenomenon leading to anterior pain and snapping, is described against coracoid and conjoint tendon [13].

The concept of glenosphere eccentricity in RSA has been developed to lower the center of rotation, aiming to prevent inferior scapular notching and increase ROM [8][9]. However, attempts have been made to modify eccentricity's position, placing it not only inferiorly but also in other directions, in order to determine which arrangement would provide the best possible ROM. Computer-based studies have been conducted to assess variations in ROM related to different glenosphere eccentricities. To the best of our knowledge, there is currently no comprehensive research evaluating the effects of different glenosphere eccentricities on internal rotation and anterior impingement.

The purpose of this study was to evaluate the influence of distalization, lateralization offset and posterior eccentricity of the glenosphere in RSA on impingement-free ROM in a virtual model. We hypothesized that posterior eccentricity would improve Hand-Behind-Back (HBB) motion and decrease the risk of anterior impingement.

Materials and methods

Study Design and Patient Population

Consecutive patients who had a computed tomography (CT) prior to RSA performed by one fellowship-trained shoulder surgeon (A.L.) were considered potentially eligible for inclusion in this retrospective analysis of data prospectively collected during the Shoulder OUTcome (SHOUT) multicenter study (ethical committee approval CCER 14-277, registration number on clinicaltrials.gov NCT02047955). Patients were included if they presented with primary osteoarthritis, cuff tear arthropathy and if they underwent RSA. Exclusion criteria were $>10^\circ$ glenoid superior inclination, $>10^\circ$ glenoid retroversion, excessive glenoid or humeral osteophytes,

previous scapula or humeral fractures, previous surgery to the index shoulder and age < 18 years old.

Shoulder Computed Tomography Data and Computational Model

This study used three-dimensional (3D) reconstructed computational models derived from CT scans. CT scans were uploaded into 3D surgical planning software to measure impingement-free ROM in various implant configurations. To standardize the positioning of the humerus and scapula across all patients, Walch A1 glenoids without deformity were selected and glenoid version and inclination were individually adjusted in each case to achieve a neutral position or the closest approximation. This 3D planning software has demonstrated its reliability in assessing the morphology of the glenoid and aiding in the precise positioning of components during shoulder arthroplasty [14].

Virtual ROM Variables

Prior to ROM simulation, virtual implantation of an RSA was executed. For the humeral component a short 135° inlay stem was selected to fit the humeral canal and neutral polyethylene cup was used. For the glenoid component, a 36-mm glenosphere was used and placed on the 25 mm baseplate at a neutral tilt and version, and a minimal seating of 75%.

Eighteen different glenosphere configurations were tested, combining two different glenosphere positions (flush with the inferior glenoid rim; inferior margin of the glenosphere 5 mm below the inferior glenoid rim), three different glenosphere eccentricity options (concentric; posteroinferior (45°), posterior (90°)), and three different lateral offset values (no offset; 3 mm offset; 6 mm offset). Based on manufacturer specifications, glenosphere eccentricity was set to 2 mm for a 36 mm diameter glenosphere. To ensure 5 mm of overhanging below the inferior glenoid rim, the distance was measured on the CT scan, bony sequences, coronal view, on the slice passing through the central axis of the central peg.

Kinematic Simulation

Measurements were conducted in the sagittal (flexion and extension) and axial (internal [IR] and external rotations [ER] with elbow at side in a neutral anatomic position) planes. Additionally, multiplanar movements such as combing hair, hand-to-contralateral, and HBB were assessed. These motions were implemented by combining elementary planes of movement (flexion/extension, abduction/adduction, and rotation) according to kinematic data of daily living tasks previously published in the literature [14][15][16]. ROM values were quantified both in degrees and as a percentage of a maximum achievable ROM according to the simulation

software's parameters. Values for hand-to-contralateral, combing hair, and HBB were simulated and recorded only as a percentage of the full ROM. Each of these parameters was presented in terms of degrees and/or percentages but at the same time visually represented by a dynamic 3D model highlighting impingement spots between the humeral and glenoid components (**Figure 1A and 1B**).

The predetermined maximum values were as follows: 100° for internal rotation, 60° for external rotation, and 120° for both flexion and extension. Any ROM simulations exceeding these predetermined thresholds were capped at 100%. ROM values below 50% were deemed inadequate.

Glenosphere to Coracoid Process and Conjoint Tendon Distance Evaluation

For each of the 18 glenosphere configurations, the distance from the glenosphere surface to the coracoid process and the conjoint tendon was also recorded.

The distance between the glenosphere surface and the coracoid process was measured through the bony sequence sagittal projection of the CT scan uploaded into the software. To standardize the measurement, the distance was always measured in the first CT image where the glenosphere appeared as a complete circle, scrolling the images from medial to lateral. The distance was calculated between the lower edge of the coracoid and the peripheral margin of the glenosphere (**Figure 2A**).

The distance from the glenosphere surface to the conjoint tendon was assessed using soft tissue sequences in the axial projection of the uploaded CT scan within the software. To ensure a standardized measurement method, the distance

was consistently measured in the CT slice passing through the central portion of the baseplate's peg. This measurement was taken from the posterior edge of the conjoint tendon (tracing it from the coracoid) to the anterior surface of the glenosphere (**Figure 2B**). In order to enhance measurement accuracy, the conjoint tendon was proximally identified at the coracoid process and then distally followed till the measurement level.

Equity, Diversity and Inclusion Statement

The studied population included women (77%) and men originating from various countries in Southern Africa, North America, Oceania and Europe in a usual proportion for such pathology. We do not present data on race, socioeconomic status or other social determinants.

Statistical Analysis

Descriptive statistics were used to summarize the data. Variables were reported as mean \pm standard deviation (SD), 95% confidence intervals (CI) and range (minimum – maximum). Comparison of two groups were made with the Wilcoxon signed-rank test, and comparison of more than two groups were made with the Friedman test. In instances where the Friedman test yielded significant results, post-hoc tests were carried out using the Wilcoxon signed-rank test, with the Holm correction applied to mitigate the potential for Type I errors arising from multiple comparisons. The statistical analyses were performed using R (version 3.6.2; R Foundation for Statistical Computing). Statistical significance was established at a threshold of $p < 0.05$.

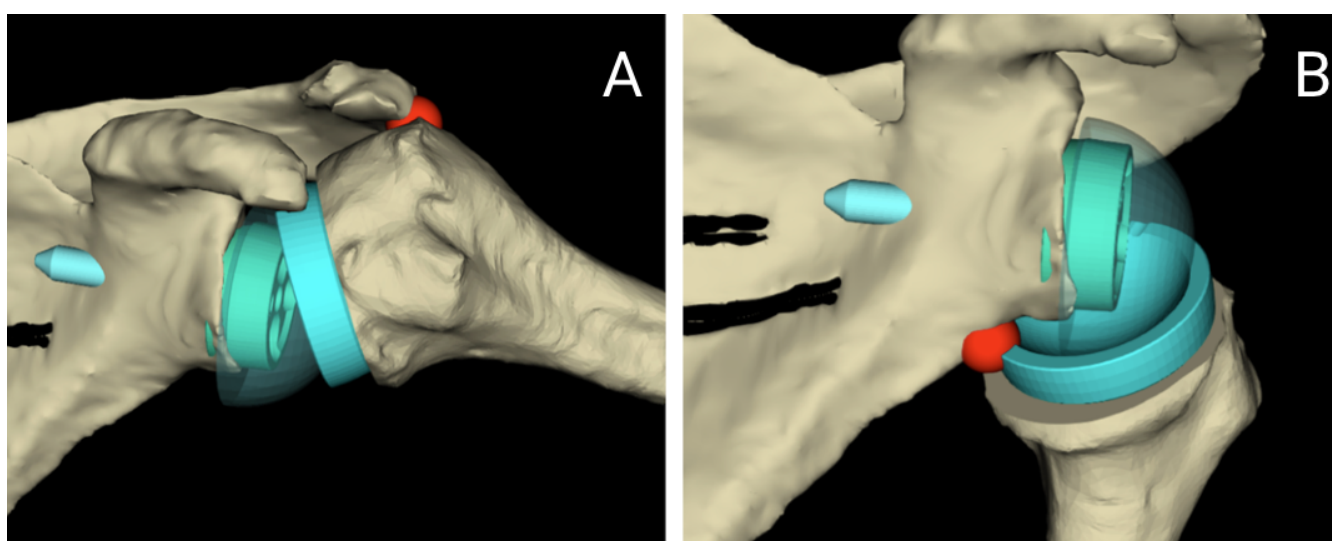


Figure 1: Screenshots showing shoulder joint dynamic 3D model highlighting abutment impingement spots during ROM. (A) adduction, (B) external rotation.

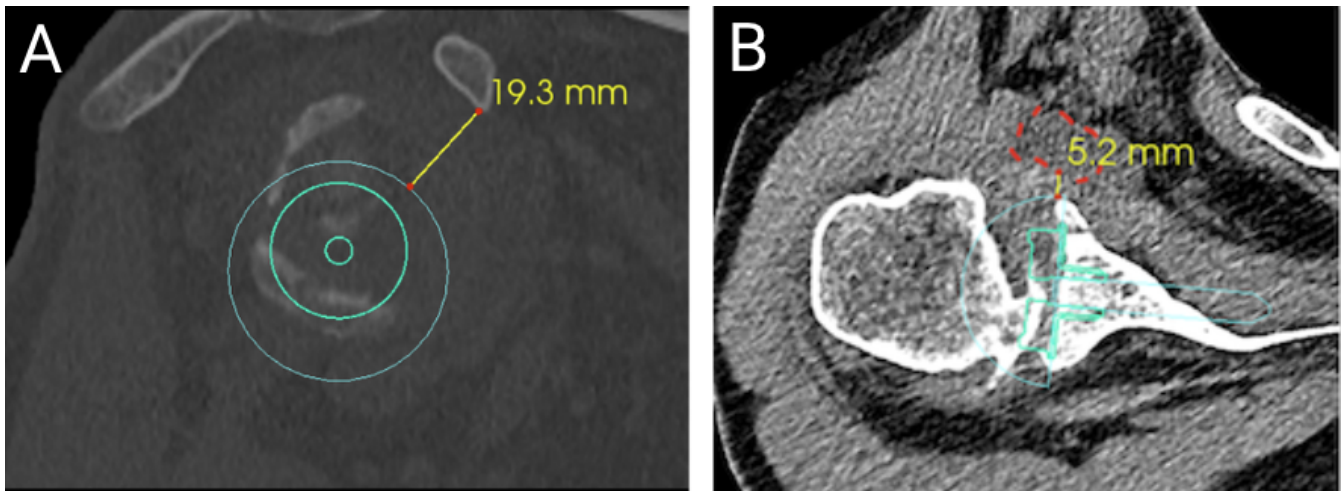


Figure 2: (A) This screenshot shows the CT scan slice where the peripheral margin of the glenosphere just appeared as a full circle, scrolling in sagittal plain from medial to lateral, on bone sequences from the CT scan uploaded to a software (Imascap, Brest, France). The distance between the coracoid's inferior pole and the peripheral margin of the glenosphere is then measured. (B) This screenshot shows the CT scan slice, axial plain, soft-tissue sequences, passing through the middle of the central baseplate's peg, where it has the biggest shape, from the CT scan uploaded to a software (Imascap, Brest, France). The red dashed line represents the conjoint tendon in cross-section. The distance between the conjoint tendon and the peripheral margin of the glenosphere is then measured.

Results

A total of 111 CT scans were screened with the 3D software. Ninety-eight were excluded from the study due to either excessive glenoid/proximal humerus osteophytes or excessive glenoid retroversion and/or superior inclination. Finally, 13 patients (3 men and 10 women) with an average age of 75,3 years were included in the study, representing 234 different computational simulations. Average glenoid retroversion and superior inclination were 7,3 and 7,6 respectively.

Sagittal plane ROM

Flexion

Compared to flush glenospheres, positioning the glenosphere inferiorly improved flexion by 8% (95%CI 7% – 10%) or 10° (95%CI 7° – 13°) ($p < 0.001$). Among inferior glenospheres, lateralizing the glenosphere increased flexion by 9% (95%CI 6% – 12%) or 11° (95%CI 6° – 15°) ($p = 0.008$) with an offset of 6 mm and by 7% (95%CI 5% – 10%) or 9° (95%CI 4° – 15°) ($p = 0.008$) with an offset of 3 mm. There was, however, no statistically significant effect of eccentricity on flexion ($p = 0.383$) (**Supplementary Figure 1**).

Extension

Compared to flush glenospheres, inferior glenospheres exhibited on average 42% (95%CI 32% – 52%) or 52° (95%CI 40° – 63°) ($p < 0.001$) greater extension. Among inferior glenospheres, both posteroinferior and posterior eccentricities yielded better extension compared to the concentric glenospheres by 15% (95%CI 7% – 23%, $p < 0.001$) or 18° (95%CI 5° – 31°) ($p < 0.001$). When considering inferior and eccentric designs, lateralizing the glenosphere increased flexion by 45% (95%CI 33% – 57%), or 54° (95%CI 40° – 68°) ($p = 0.001$) with an offset of 6 mm and by 18% (11% – 25%) or 26° (95%CI 14° – 39°) ($p < 0.001$) with an offset of 3 mm (**Supplementary Figure 1**).

Transverse Plane ROM

Internal Rotation with elbow at side (IR)

Compared to flush glenospheres, positioning the glenosphere inferiorly improved IR by 38% (95%CI 33% – 43%) or 38° (95%CI 33° – 43°) on average ($p < 0.001$). Among inferior glenospheres, concentric designs exhibited a statistically higher IR than posterior by 11% (95%CI 9% – 13%) or 11° (95%CI 9° – 13°) ($p < 0.001$) and posteroinferior by 5% (95%CI 4% – 6%) or 5° (95%CI 4° – 6°) ($p < 0.001$) eccentricities. When considering inferior and concentric glenospheres, there was no effect of glenosphere lateralization ($p = 0.215$) (**Supplementary Figure 2**).

External Rotation (ER)

Compared to flush glenospheres, inferior glenospheres showed higher ER by 44% on average (95%CI 39% – 49%) or 26° (95%CI 24° – 29°) ($p < 0.001$). The posteroinferior and

posterior eccentricities designs respectively demonstrated better ER compared to concentric glenospheres by 10% (95%CI 9% – 12%) or 5° (95%CI 4° – 6°) ($p < 0.001$) and 9% (95%CI 6% – 11%) or 5° (95%CI 4° – 6°) ($p < 0.001$). When considering inferior and eccentric designs, lateralizing the glenosphere increased ER by 23% (95%CI 17% – 30%) or 14° (95%CI 10° – 18°) ($p < 0.001$) with an offset of 6 mm and by 15% (11% – 20%) or 9° (95%CI 7° – 12°) ($p < 0.001$) with an offset of 3 mm (**Supplementary Figure 2**).

Multi-plane Movements ROM

HBB

Compared to flush glenospheres, inferior glenospheres yielded higher HBB by 15% on average (95%CI 12% – 18%, $p < 0.001$). Among inferior designs, there was no effect of eccentricity ($p = 0.135$) or lateral offset ($p = 0.095$) on HBB (**Supplementary Figure 3**).

Hand-to-contralateral

Compared to flush glenospheres, inferior glenospheres yielded greater hand-to-contralateral motion by 51% (95%CI 45% – 58%, $p < 0.001$) on average. Among inferior designs, concentric glenospheres exhibited greater hand-to-contralateral motion compared to posterior by 28% (95%CI 17% – 39%, $p < 0.001$) and posteroinferior by 8% (95%CI 2% – 14%, $p = 0.004$) eccentricities. No statistically significant differences, however, were found between different levels of lateral offset for glenospheres that were both inferior and concentric ($p = 0.165$) (**Supplementary Figure 3**).

Combing Hair

Compared to flush glenospheres, inferior glenospheres had greater combing hair motion by 6% (95%CI 5% – 7%, $p < 0.001$) on average. Among inferior glenospheres, combing hair did not statistically differ between the different eccentric ($p = 0.368$) or lateral offset ($p = 0.368$) designs (**Supplementary Figure 3**).

Distance from Glenosphere to Anatomical Structures

Coracoid Process

Compared to flush glenospheres, positioning the glenosphere inferiorly increased the distance to the coracoid process by 2.6 mm on average (95%CI 2.3mm – 2.9mm, $p < 0.001$). Among inferior glenospheres, eccentric designs had a greater distance to the coracoid process compared to concentric designs by 1.6 mm (95%CI 1.1mm – 2.0mm, $p < 0.001$) if posterior and by 1.3 mm (95%CI 1.1mm – 1.5mm, $p < 0.001$) if posteroinferior. Among inferior and eccentric glenospheres, a lateral offset tended to slightly improve the distance to the coracoid process but did not reach statistical significance ($p = 0.056$) (**Supplementary Figure 4**).

Conjoint Tendon

Compared to inferior glenospheres, flush designs had a greater distance to the conjoint tendon by 0.7 mm on average (95%CI 0.4mm – 1.1mm, $p < 0.001$). In flush glenospheres, posterior and posteroinferior eccentricities increased the distance to the conjoint tendon by 1.1 mm and 1.0 mm, respectively, compared to concentric designs ($p < 0.001$ and $p = 0.002$). Among inferior glenospheres, eccentric designs were at a greater distance from the conjoint tendon by 1.3 mm (95%CI 0.8mm – 1.8mm, $p < 0.001$) for posterior glenospheres and by 1.1 mm (95%CI 0.8mm – 1.5mm, $p < 0.001$) for posteroinferior glenospheres compared to concentric designs. There was, however, no effect of lateral offset on the distance to the conjoint tendon neither among flush eccentric designs ($p = 0.735$) nor among inferior eccentric designs ($p = 0.213$) (**Supplementary Figure 4**).

Best combinations

Out of the 18 configurations, 9 (50%) provided an average ROM in all directions of at least 50% and all of them (100%) comprised an inferior glenosphere (**Figure 3 and 4**). Among the top 5 configurations regarding ROM, two were considered not optimal (concentric designs) given they were associated with shorter distances to the conjoint tendon and coracoid process. Three configurations showed optimal performance: 1) inferior glenosphere with posteroinferior eccentricity and 6 mm of lateral offset, 2) inferior glenosphere with posteroinferior eccentricity and 3 mm lateral offset, and 3) inferior glenosphere with posterior eccentricity and 6 mm of lateral offset (**Table 1, Figure 4**).

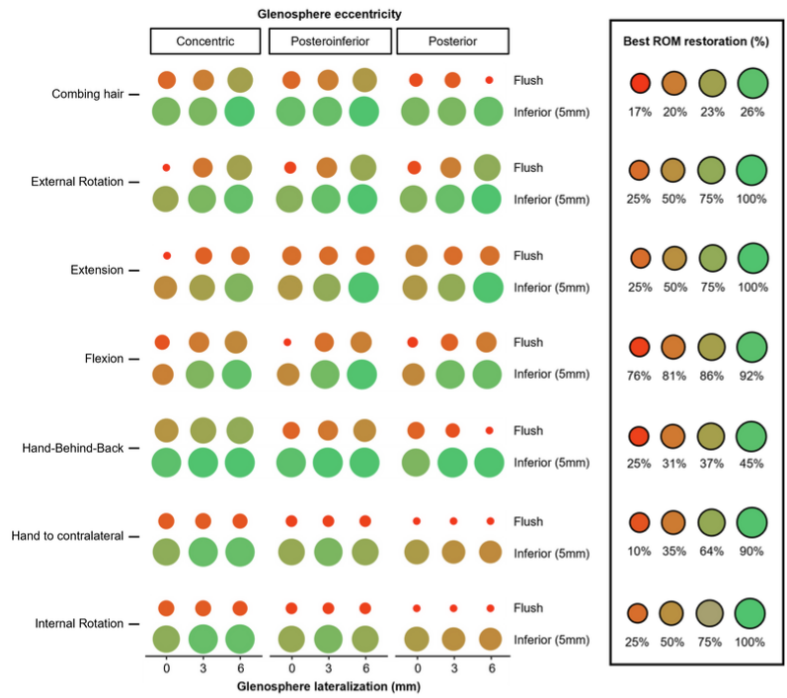


Figure 3: Mean level (%) of healthy ROM restoration for the 18 different glenosphere designs.

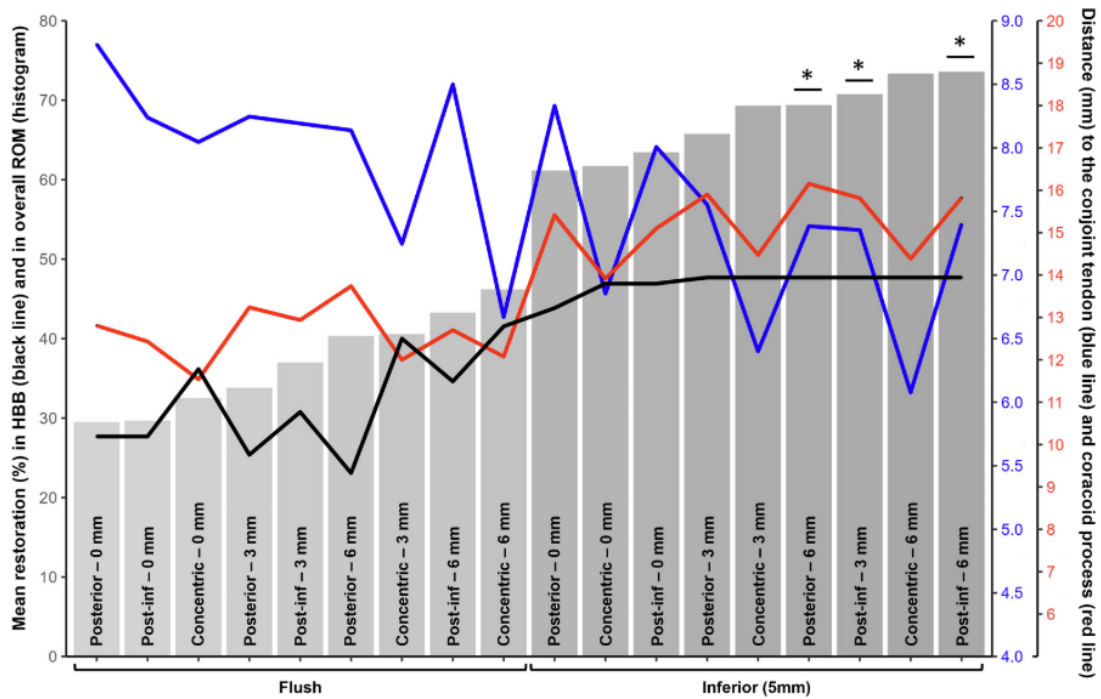


Figure 4: Mean overall restoration of healthy ROM for the 18 different glenosphere configurations (bars). The lines indicate, for each configuration, the distance between the glenosphere and the conjoint tendon (blue) and coracoid process (red) as well as and HBB (black). The asterisks indicate the three configurations considered the best for their good ROM restoration and distances to the conjoint tendon and coracoid process.

Table 1: Summary of outcomes for the three optimal glenosphere configurations

	Inferior border (5mm)		
	Posteroinferior eccentricity		Posterior eccentricity
Outcomes	6mm lateral offset	3mm lateral offset	6mm lateral offset
Glenosphere distance, mm			
With conjoint tendon	7 ±2	7 ±2	7 ±3
With coracoid process	16 ±4	16 ±3	16 ±4
Range of motion restoration*, %			
Combing hair	26 ±2	26 ±5	26 ±3
Hand behind back (HBB)	48 ±4	48 ±4	48 ±4
Hand-to-contralateral	67 ±38	77 ±37	46 ±39
External rotation	98 ±5	92 ±11	98 ±5
Internal rotation	83 ±11	86 ±11	77 ±13
Extension	100 ±0	76 ±32	100 ±0
Flexion	92 ±9	91 ±9	91 ±10
Overall range of motion restoration*, %	74 ±28	71 ±25	69 ±30

Values are mean ± standard deviation (SD). * Restoration compared to the healthy shoulder.

Discussion

The main findings of the present study were that glenospheres implanted 5 mm inferiorly with a posteroinferior eccentricity and lateral offset provide improved ROM, including HBB, in a virtual model. In addition, these glenosphere configurations generate an increased glenosphere-to-coracoid process and glenosphere-to-conjoint tendon distances, limiting potentially anterior impingements. We observed only minor improvement in HBB, probably related to a worsening of IR when the eccentricity becomes more posterior. Hand-behind-back includes extension, abduction, and internal rotation. Posteroinferior or posterior eccentricities improved only the former two but worsened the latter, explaining probably why our hypothesis is only partially confirmed.

Bony Impingements

The present study analyzed multiplanar motions such as HBB motion to attempt to simulate real activities of daily

living. Improvement (15%) was reached through glenosphere 5 mm inferior overhang ($p<0,001$) without noticeable influence of baseplate lateral offset ($p=0.095$). Arenas-Miquelez et al. [10] studied the impact of humeral and glenoid component variations not only on a single direction but on the whole ROM in RSA through a computer model study. They also analyzed 13 shoulder CT scans, virtually implanting different combinations of humeral and glenoid components. Regarding glenosphere eccentricity, they did not find statistically significant differences through total global ROM, whether the eccentricity was concentric, 2 mm inferior, or 2 mm posteroinferior. Like in the present study, they reported with an inferior eccentricity configuration a significant better adduction and internal rotation compared to concentric and posteroinferior eccentricity. Similarly, Huish et al. [17] was found that IR was improved by isolated glenosphere inferior overhang (5 mm) ($p<0,001$). Xu et al. [11] demonstrated in a computational study that posteroinferior eccentricity significantly increases ROM in external rotation compared to concentric glenosphere and antero-inferior eccentricity ($p<0.05$). It seems thus that, in computer models, inferior

eccentricity improves internal rotation and posterior eccentricities improve extension and external rotation, thanks to a posterior shift of the center of rotation [18]. Clinically, however, Pak et al. [12] suggested that a posteroinferior glenosphere position may improve ROM including internal rotation at two years follow-up when using a 135 inlay humeral component and a lateralized glenoid.

Soft Tissue Impingements

Postoperative anterior impingement is an under reported complication that is a cause of IR limitation and anterior pain. (4) It may also impact subscapularis healing, another key factor for hand-behind-back motion [19]. In the current study glenosphere-to-coracoid and glenosphere-to-conjoint tendon distances were measured to assess for potential anterior impingement. Posteroinferior and posterior eccentricities increased the distances to these structures, potentially reducing impingement and thus increasing range of certain movements. Specifically, eccentricity improved extension and external rotation. As shown by Pak et al. in a clinical study [12], posteroinferior glenosphere position may improve IR as well when using a similar 135° inlay humeral component. The latter results have been confirmed by the one published by Klosterman et al. [20]. Their retrospective review of a multicenter clinical registry of RSAs with a minimum follow-up of two years aimed to understand the cause of postoperative anterior pain associated with IR deficit. They highlighted a direct proportionality between the subcoracoid distance, defined as the distance between the posterior aspect of the coracoid and the anterior glenosphere on the axillary radiograph, and IR both with the arm at 0° and 90° abduction; for every additional millimeter of subcoracoid distance, an improvement in HBB were gained ($p < 0.001$) and 6° of IR ($p = 0.034$). These results are not consistent with those found in the present study in which internal rotation decreased with posteroinferior and posterior eccentricities. However, it should be noted that in Klosterman's study, all different implants had lateralized glenospheres, whereas, in the present study, we examined both standard and lateralized glenospheres (0 mm, +3 mm, +6 mm). In addition, in the present study glenoid lateralization did not result in internal rotation improvements ($p = 0.215$) and neither had any effect on increasing glenosphere-to-coracoid/conjoint tendon distance ($p = 0.056$ and $p = 0.751$ for coracoid and conjoint tendon, respectively). Finally, the current study was a virtual simulation, which cannot account for soft tissue tension. It is possible that the soft tissue tension plays a significant role in limiting IR.

Limitations

The limitations include those inherent to computer-based models. First, the software used may not be a valid *in vivo* representation of ROM due to predetermined scapular positioning and the exclusion of soft tissue considerations [21]. This may account for discrepancies between the reported ROM and what is observed clinically [22]. Second, clinical recommendations cannot be extrapolated as there may be consequences to inferior positioning such as risk of nerve injury or increased tension on the acromion leading to stress fracture. Third, we evaluated glenohumeral ROM but could not consider rotator cuff status [23] and scapulothoracic movements [24][19], key factors for HBB motion [19]. Fourth, the CT used allowed us to implant 36 mm glenospheres only and we chose an inlay design with a prosthetic inclination of 135°, and concern mainly female patients (77%): our findings may not be generalizable. Fifth, the distance from glenosphere to anatomical structures were evaluated in a preoperative configuration. In fact, in postoperative condition, shoulder's center of rotation is distalized after RSA [25], thus causing an increased tension of the conjoint tendon, which, as a cord effect, moves closer to the anterior margin of the glenoid. Consequently, our soft tissue measurements might be overestimated. Sixth, we had to exclude a consequent number of shoulders due to version/inclination parameters and exuberant osteophytes. Seventh and lastly, during different configuration testing, precise glenosphere eccentricity orientation was set. Intraoperatively, reaching the right degrees might a real challenge without precise navigation system [26]. In light of the above, our findings certainly require clinical correlation.

Conclusions

In a virtual simulation model with a 135° inlay humeral component, posteroinferior eccentricity and lateral offset optimizes ROM in all directions, including HBB. Posterior or posteroinferior eccentricity may reduce anterior impingement risk by increasing the clearance from the coracoid process and conjoint tendon.

Open access statement

This is an open-access article distributed under the terms of the Creative Commons Attribution Non-Commercial (**CC BY-NC 4.0**), see <https://creativecommons.org/licenses/by-nc/4.0/> licence, which permits the sharing and adapting work, as long as it is for non-commercial purposes and proper credit is given to the original creator.

Source of funding

This study was funded by a grant from FORE (Foundation for research and teaching in the field of orthopedic surgery, trauma, sports medicine, and imaging of the musculoskeletal system). Grant # FORE 2024-16.

Conflict of interest

AG, AE, AP and HB: received no financial or material support for the research, authorship, and/or publication of this article. PJD: discloses receipt of the following financial or material support for the research, authorship, and/or publication of this article: he received royalties from and is a consultant and paid speaker for Arthrex. He is the co-founder of Med4Cast. PC: discloses receipt of the following financial or material support for the research, authorship, and/or publication of this article: he receives royalties from and is a consultant and paid speaker for Stryker and Enovis. He is the co-founder of Med4Cast and Follow. He is on the board of SECEC and IBSES. AL: discloses receipt of the following financial or material support for the research, authorship, and/or publication of this article: he is a paid consultant for Medacta, and Enovis. He received royalties from Stryker and Medacta. He is the (co-)founder of FORE, Med4Cast, and BeeMed. He owns stock options in Medacta and Follow Health. He is on the board of the French Arthroscopic Society.

Author's contributions:

AG: Data acquisition and analysis, writing article. PJD: Study design, analysis and interpretation of data, and reviewed article. PC: Study design and reviewed article. AE: Data acquisition, writing article. AP: Statistics, illustrations, reviewing article. HB: Statistics, illustrations, reviewing article, coordination. AL: Study design, supervision, founding, writing and reviewed article.

Acknowledgments

The authors thank the LaTour (Leading Advancements in Therapeutic and Outcome-based Research) group for their support.

References

1. Chamberlain AM, Aleem AW, Sefko JA, Steger-May K, Keener JD. Clinical outcomes after reverse shoulder arthroplasty in patients 60 years old and younger; medium-term results. *JSES Int.* 2023;7(2):277-84. doi: 10.1016/j.jseint.2022.12.018
2. Kim JY, Rhee YG, Rhee SM. Clinical Outcomes after Reverse Total Shoulder Arthroplasty According to Primary Diagnosis. *Clinics in orthopedic surgery.* 2020;12(4):521-8. doi:10.4055/cios19164

3. Collin P, Rol M, Muniandy M, Gain S, Ladermann A, Ode G. Relationship between postoperative integrity of subscapularis tendon and functional outcome in reverse shoulder arthroplasty. *J Shoulder Elbow Surg.* 2021. 10.1016/j.jse.2021.05.024
4. Cunningham G, Lädermann A. Redefining anterior shoulder impingement: a literature review. *International orthopaedics.* 2017. doi: 10.1007/s00264-017-3515-1
5. Lädermann A, Denard PJ, Boileau P, Farron A, Deransart P, Terrier A, et al. Effect of humeral stem design on humeral position and range of motion in reverse shoulder arthroplasty. *International orthopaedics.* 2015;39(11):2205-13. doi: 10.1007/s00264-015-2984-3
6. Lädermann A, Denard PJ, Boileau P, Farron A, Deransart P, Walch G. What is the best glenoid configuration in onlay reverse shoulder arthroplasty? *International orthopaedics.* 2018;42(6):1339-46. doi: 10.1007/s00264-018-3850-x
7. Lädermann A, Denard PJ, Collin P, Zbinden O, Chiu JC, Boileau P, et al. Effect of humeral stem and glenosphere designs on range of motion and muscle length in reverse shoulder arthroplasty. *International orthopaedics.* 2020;44(3):519-30. doi: 10.1007/s00264-019-04463-2
8. Lädermann A, Denard PJ, Tirefort J, Collin P, Nowak A, Schwitzgubel AJ. Subscapularis- and deltoid-sparing vs traditional deltopectoral approach in reverse shoulder arthroplasty: a prospective case-control study. *Journal of orthopaedic surgery and research.* 2017;12(1):112. doi: 10.1186/s13018-017-0617-9
9. Lädermann A, Lo EY, Schwitzgubel AJ, Yates E. Subscapularis and deltoid preserving anterior approach for reverse shoulder arthroplasty. *Orthopaedics & traumatology, surgery & research : OTSR.* 2016;102(7):905-8. DOI: 10.1016/j.otsr.2016.06.005
10. Arenas-Miquelez A, Murphy RJ, Rosa A, Caironi D, Zumstein MA. Impact of humeral and glenoid component variations on range of motion in reverse geometry total shoulder arthroplasty: a standardized computer model study. *J Shoulder Elbow Surg.* 2021;30(4):763-71. doi: 10.1016/j.jse.2020.07.026
11. Xu X, Sun Q, Liu Y, Wang D, Diao S, Wang H, et al. Comparative Analysis of Eccentric Glenosphere in Reverse Total Shoulder Arthroplasty: A Computer Simulation Study. *Int J Gen Med.* 2023;16:4691-704. doi: 10.2147/IJGM.S426191
12. Pak T, Ardebol J, Kilic AI, Sears BW, Lederman E, Shoulder Arthroplasty Research Committee g, et al. Posteroinferior Glenosphere Positioning is Associated with Improved Range of Motion Following Reverse Shoulder Arthroplasty with a 135 degrees Inlay Humeral Component and Lateralized Glenoid. *J Shoulder Elbow Surg.* 2024. doi: 10.1016/j.jse.2024.02.019
13. Fleet CT, Carroll P, Johnson JA, Athwal GS. Reverse shoulder arthroplasty implant design and configuration has a significant effect on conjoint tendon impingement. *J Shoulder Elbow Surg.* 2025;34(6):1487-97. DOI: 10.1016/j.jse.2024.10.006
14. Cai L, Ma Y, Xiong S, Zhang Y. Validity and Reliability of Upper Limb Functional Assessment Using the Microsoft Kinect V2 Sensor. *Appl Bionics Biomech.* 2019;2019:7175240. doi:10.1155/2019/7175240
15. Namdari S, Yagnik G, Ebaugh DD, Nagda S, Ramsey ML, Williams GR, Jr., Mehta S. Defining functional shoulder range of motion for activities of daily living. *J Shoulder Elbow Surg.* 2012;21(9):1177-83. doi:10.1016/j.jse.2011.07.032

16. Rundquist PJ, Obrecht C, Woodruff L. Three-dimensional shoulder kinematics to complete activities of daily living. *American journal of physical medicine & rehabilitation / Association of Academic Physiatrists*. 2009;88(8):623-9. DOI: 10.1097/PHM.0b013e3181ae0733
17. Huish EG, Jr., Athwal GS, Neyton L, Walch G. Adjusting Implant Size and Position Can Improve Internal Rotation After Reverse Total Shoulder Arthroplasty in a Three-dimensional Computational Model. *Clin Orthop Relat Res*. 2021;479(1):198-204. DOI: 10.1097/CORR.0000000000001526
18. Bauer S, Meylan A, Mahloulou J, Shao W, Blakeney WG. Dialing the glenosphere eccentricity posteriorly to optimize range of motion in reverse shoulder arthroplasty. *JSES Int*. 2025;9(1):181-7. DOI: 10.1016/j.jseint.2024.09.003
19. Collin P, Nabergoj M, Ode G, Denard PJ, Gain S, Bothorel H, Ladermann A. Functional internal rotation is associated with subscapularis tendon healing and increased scapular tilt after Grammont style bony increased offset reverse shoulder arthroplasty with 155 degrees humeral implant. *J Shoulder Elbow Surg*. 2025;34(3):768-77. DOI: 10.1016/j.jse.2024.04.023
20. Klosterman EL, Tagliero AJ, Lenters TR, Denard PJ, Lederman E, Gobezie R, et al. The subcoracoid distance is correlated with pain and internal rotation after reverse shoulder arthroplasty. *JSES Int*. 2024;8(3):528-34. doi: 10.1016/j.jseint.2024.01.010
21. Walch G, Vezeridis PS, Boileau P, Deransart P, Chaoui J. Three-dimensional planning and use of patient-specific guides improve glenoid component position: an in vitro study. *J Shoulder Elbow Surg*. 2015;24(2):302-9. DOI: 10.1016/j.jse.2014.05.029
22. Thomas LG, Chalmers PN, Henninger HB, Davis EW, Tashjian RZ. Preoperative Planning Software Does Not Accurately Predict Range of Motion in Reverse Total Shoulder Arthroplasty. *J Am Acad Orthop Surg*. 2024;32(8):e378-e86. DOI: 10.5435/JAAOS-D-23-00519
23. Adam MF, Ladermann A, Denard PJ, Lacerda F, Collin P. Preoperative diagnosis and rotator cuff status impact functional internal rotation following reverse shoulder arthroplasty. *J Shoulder Elbow Surg*. 2024;33(7):1570-6. doi: 10.1016/j.jse.2023.11.020
24. Moroder P, Akgun D, Plachel F, Baur ADJ, Siegert P. The influence of posture and scapulothoracic orientation on the choice of humeral component retrotorsion in reverse total shoulder arthroplasty. *J Shoulder Elbow Surg*. 2020;29(10):1992-2001. DOI: 10.1016/j.jse.2020.01.089
25. Lädermann A, Williams MD, Mélis B, Hoffmeyer P, Walch G. Objective evaluation of lengthening in reverse shoulder arthroplasty. *J Shoulder Elbow Surg*. 2009;18(4):588-95. DOI: 10.1016/j.jse.2009.03.012
26. Rojas JT, Menzemer J, Rashid M, Hayoz A, Ladermann A, Zumstein MA. Navigated augmented reality through a head-mounted display leads to low deviation between planned, intra- and post-operative parameters during glenoid component placement of reverse shoulder arthroplasty: a proof-of-concept case series. *J Shoulder Elbow Surg*. 2024. DOI: 10.1016/j.jse.2024.05.006